

HZPP-9801  
Jan 5, 1998

# THE CONTRIBUTION OF REGGEON IN CHARGE EXCHANGE PROCESSES

Zhou Yufeng<sup>1</sup> Peng Hongan<sup>2</sup> Liu Lianshou<sup>1</sup>

## Abstract

We discuss in this paper The experimental results on maximum psedo-rapidity  $\eta_{max}$  distribution in the charge exchange process  $e + p \rightarrow e + n + X$  in ZEUS Collaboration at HERA. We calculate the contributions of  $\mathcal{R}_\rho$ ( $\rho$ -Reggeon associated with  $\rho$  meson) from regge phenomenology and  $\pi^+$ -exchange from pion cloud model. The results show that neither the  $\mathcal{R}_\rho$ -exchange nor the pion cloud model alone can explain the experimental data well, but after considering both these two processes together, by using Monte Carlo simulation, a good agreement between theoretical results and experimental data is found. This means that in discussing the large rapidity gap phenomena in deep inelastic scattering, both of the two processes play substantial role.

**Keywords:** Reggeon-exchange, large rapidity gap, pion-exchange

<sup>1</sup> Institute of Particle Physics, Huazhong Normal University, Wuhan 430079 China

<sup>2</sup> Department of Physics, Peking University, Beijing 100871 China

# 1 Introduction

In recent years, the observation of large rapidity gap (LRG) events from ZUES and H1[1] collaborations in HERA has attracted much interest. This class of events can not be predicted from standard deep inelastic scattering (DIS) which assumes that a colored quark was stuck by lepton, so that there is a color field between the proton remnant and the stuck quark, and particles will be produced in the whole region between them. On the other hand, large rapidity gap means that there is little energy deposited in the forward region. In terms of rapidity distribution this means that there is a large gap between the produced particles and the beam remnant. The ratio of the frequency of large rapidity gap events to that of normal DIS events is about 10%.

The LRG events suggest that in these processes, a color singlet object is exchanged. One of the most probable candidate of this object is Pomeron( $\mathcal{IP}$ ), ie. the Regge trajectory with the quantum number of vacuum. In the process of Pomeron exchange the proton is diffractively scattered into the forward region and separated from the other particles in rapidity. The models based on Pomeron exchange such as the I-S model[2], D-L model[3] have made great success on describing the properties of LRG events.

Since pomeron is one of the many Reggeon trajectories, one may go further to ask what about the contribution of other Regge trajectories in strong interaction. In  $e + p$  forward hard diffractive scattering process, Beside the contribution of pomeron, other reggeon exchange such as  $\rho_0$ -reggeons, and the  $\pi^0$  meson exchange must be considered, although their contribution to the cross section are about one or two order of magnitude smaller than that of pomeron exchange.

But, as we know, there is a significant difference between pomeron and other Reggeons. The  $\mathcal{IP}$  has the quantum number of vacuum, the other Reggeons have quantum numbers of the particles which belong to the corresponding Regge trajectories. So  $\mathcal{IP}$ -exchange and Reggeon-exchange may occur in different processes. If we can isolate some process of Reggeon-exchange from that of  $\mathcal{IP}$  ones, we will get the opportunity of studying the properties of Reggeon-exchange. In [4] the  $\mathcal{IR}_\rho$ -exchange (the exchange of  $\rho$ -Reggeon associated with  $\rho$  meson) was studied. Since the  $\mathcal{IR}_\rho$  has the quantum number of  $\rho^+$ , the  $\mathcal{IR}_\rho$ -exchange process is a charge exchange process. In the case of  $\mathcal{IP}$ -exchange, no charge was exchanged. So in  $\mathcal{IP}$ -exchange we will find the outgoing proton in forward direction. On the contrary, in  $\mathcal{IR}_\rho$ -exchange the final forward hadron is a neutron. Recently a forward neutron calorimeter (FNC) was

installed in ZEUS Collab. in HERA, which can detect the fast neutron in forward region, so the charge exchange process can be separated from neutral current process.

In this paper we first present the formalism of  $\mathcal{R}_\rho$ -exchange in section 2. Then, for a comparison the process of  $\pi^+$ -exchange from pion cloud model was also discussed in section 3. In section 4, we use Monte Carlo method to study the exclusive properties of these two process. The  $\eta_{max}$  distribution is obtained. From the comparison to the experimental data, we find that neither the  $\mathcal{R}_\rho$ -exchange nor the  $\pi^+$ -exchange alone can describe the data, but combining these two processes together, the experimental data can be explained very well.

## 2 The formalism of $\mathcal{R}_\rho$ -exchange

The  $\mathcal{R}_\rho$ -exchange has been studied in  $\pi$ - $N$  interaction[5]. In the reaction:

$$\pi^- + P \rightarrow \pi^0 + N \quad (1)$$

only the  $\rho^+$ -Regge trajectory (with quantum numbers  $J^{pc} = 1^{--}$ ) can be exchanged. In Regge theory the  $s$ -channel helicity amplitudes has the form[6]:

$$A_{H_s}(s, t) \xrightarrow{s \gg m_N^2} \left(\frac{-t}{2m_N^2}\right)^{\frac{1}{2m}} \left(\frac{1 - e^{-i\pi\alpha_\rho(t)}}{\sin\alpha_\rho(t)}\right) \left(\frac{s}{2m_N^2}\right)^{\alpha_\rho(t)} \gamma_\pi(t) \gamma_{\mu_2\mu_4}(t), \quad (2)$$

where  $A_{H_s}$  is the  $s$ -channel helicity amplitudes,  $s$  is the energy squared in cms frame,  $m_N$  is the mass of nucleon,  $t$  is the four momentum transfer squared,  $\alpha_\rho(t)$  is the Regge trajectory of  $\rho^+$ .  $\gamma_\pi, \gamma_{\mu_2\mu_4}(t)$  are vertex functions of  $\mathcal{R}_\rho\pi\pi$  and  $\mathcal{R}_\rho NN$  respectively.  $m$  is defined as:

$$m \equiv |\mu_2 - \mu_4|. \quad (3)$$

$\mu_2, \mu_4$  are helicities of the initial proton and final neutron, see Fig.1. Since in diffractive interaction  $t$  is very small, we set  $m=0$  [4]. The differential and total cross section can be written as:

$$\frac{d\sigma}{dt}(s, t) = \frac{1}{64\pi sk^2} \frac{1}{2} \sum |A_{H_s}(s, t)|^2, \quad (4)$$

$$\sigma_{tot} = 2\beta_\rho^2 \left(\frac{s}{2m_N^2}\right)^{\alpha(0)-1} \quad (5)$$

respectively, where  $k \equiv p_{c.m}^\pi$  is the momentum of pion in  $\pi$ - $N$  cms frame,  $\beta_\rho$  is the coupling function between  $\mathcal{R}_\rho$  and light quarks (u,d quarks). From the  $\pi$ - $N$

phenomenology the  $\beta_\rho$  can be estimated as[4]:

$$\beta_\rho(t)|_{t=0} = 2.07 \text{ GeV}^{-1}. \quad (6)$$

The  $\alpha_\rho(t)$  can be written approximately as:

$$\alpha_\rho(t) = \alpha_\rho(0) + \alpha'_\rho t, \quad (7)$$

where  $\alpha_\rho(0) \approx 0.5$ ,  $\alpha'_\rho \approx 0.9 \text{ GeV}^{-2}$ . Thus, the effective propagator of  $\mathcal{IR}_\rho$  is :

$$D_\rho(t) = 2\beta_\rho^2 F_N(t) \left( \frac{s}{2m_N^2} \right)^{\frac{1}{2}(\alpha_\rho(t)-1)} \left( \frac{1 - e^{-i\pi\alpha_\rho(t)}}{\sin \pi\alpha_\rho(t)} \right), \quad (8)$$

where  $F_N(t)$  is the form factor for a quark in nucleon. It can be parameterized as follow:

$$F_N(t) = \frac{4m_N^2 - 2.8t}{4m_N^2 - t} \left( \frac{1}{1 - \frac{t}{0.7}} \right)^2. \quad (9)$$

Like the case of pomeron, it is also possible for the Reggeons to have partonic structure, i.e. it would appear in hard subprocess. In [4], the process sketched in Fig.2a was evaluated by using effective propagator and the coupling constant of  $\mathcal{IR}_\rho$ . The problem was handled very similar to the D-L model for  $\mathcal{IP}$ , where the coupling between  $\mathcal{IP}$  and the quarks is point-like. In the process of charge-exchange photo production quark-pair process :

$$\gamma^* + P \rightarrow n + q_u + \bar{q}_d, \quad (10)$$

the invariant amplitude is expressed as :

$$M = D_\rho(t) [Q_u \bar{u}_u(k) \gamma_\mu \frac{i(\not{q} - \not{k}')}{(q' - k')^2} \gamma_\rho v_d(k') + Q_d \bar{u}_u(k) \gamma_\rho \frac{i(\not{q} - \not{k}')}{(q - k')^2} \gamma_\mu v_d(k')] \bar{u}_d(p') \gamma_\rho u_u(p), \quad (11)$$

where  $Q_u = \frac{2}{3}e$ ,  $Q_d = \frac{-1}{3}e$  is the charge of  $u, d$  quark respectively. The corresponding cross section  $\sigma_{\gamma^* P}^T$  is :

$$\sigma_{\gamma^* P}^T(s, Q^2) = \frac{1}{4q_{s12}\sqrt{s}} \int \sum |M|^2 (2\pi)^4 \delta^4(p + q - p' - k - k') \frac{d^3 p'}{(2\pi)^3 2E_{p'}} \frac{d^3 k}{(2\pi)^3 2E_k} \frac{d^3 k'}{(2\pi)^3 2E_{k'}}. \quad (12)$$

Thus, the contribution to the structure function  $F_2(x, Q^2)$  can be evaluated under the equivalent photon approximation:

$$F_2(x, Q^2) = \frac{Q^2}{4\pi^2 \alpha_{em}} \sigma_{\gamma^* P}^T(s, Q^2). \quad (13)$$

### 3 The $\pi^+$ -exchange in pion cloud model

Recently the concept of pion cloud in nucleon becomes very successful in understanding the Grotfried sum rule violation observed by the New Muon Collaboration and the Drell-Yan asymmetry measured in NA51 at CERN [7].

In the charge exchange process, it is well known that the  $\pi^+$ -exchange process of pion cloud model[8] gives the largest contribution. The formalism of pion-exchange was proposed many years ago[9]. In recent years, since FNC has been installed on ZEUS Collab., one can study this process experimentally and get a very good chance to study the structure of pion. Some methods have been proposed to measure the pion structure function on HERA[10].

The process of  $\pi^+$ -exchange is sketched in Fig.3a and Fig.3b. The cross section is factorized into [11]:

$$\frac{dF_2^p}{dt dz} = f_{\pi N}(z, t) F_2^\pi(x_\pi, Q^2), \quad (14)$$

where  $f_{\pi N}(z, t)$  is the flux factor,  $F_2^\pi$  is the structure function of pion,  $z$  is the ratio of the neutron to proton light-cone momenta,  $x_\pi$  is the Bjorken variable for the pion,  $x_\pi = x/(1 - z)$ . The flux factor for Fig.3a can be expressed as [11] :

$$f_{\pi N}(z, t) = \frac{2g_\pi^2}{16\pi^2} \frac{|t|}{(m_\pi^2 - t)^2} G_1^2(t)(1 - z). \quad (15)$$

In[11], the factor  $(1 - z)$  is changed into  $(1 - z)^{1+2\alpha'_\pi|t|}$ . where  $\alpha'_\pi$  is the slop of the  $\pi$ -Regge trajectory,  $\alpha'_\pi \approx 1$ . This approach is wildly used to 'reggeize' the  $\pi$ -exchange process when  $(1 - z)$  is very small or  $|t|$  is very large[13][11]. In this kinematical region the off-shell behavior of pion should be considered [14]. But since the  $\pi$ -exchange is in the kinematical region  $z \approx 0.7 - 0.9$  and  $|t| \leq 0.2 \approx 0.4 \text{ GeV}^2$ [11], the influence of 'reggeize' is insignificant in this process. So we choose  $(1 - z)$  instead of  $(1 - z)^{1+2\alpha'_\pi|t|}$ , in consistence with the on shell-pion structure function, going to be used in the following discussion. Because the difference is important only in very limited region of phase space, both approaches lead to almost the same result[13][11].

The value of  $\pi NN$  coupling constant  $g_\pi$  is fixed at  $g_\pi^2/4\pi = 13.75$ .  $m_\pi$  is the mass of pion,  $G_1(t)$  is the form factor, which has the form  $G_1(t) = \exp[R_1^2(t - m_\pi^2)]$ , where  $R_1^2 = 0.3 \text{ GeV}^{-2}$ . The flux factor of Fig.3b has different form[11]. From[11], we know that the contribution of Fig.3b is less than that of Fig.3a for about one order of magnitude. It will not be so important in the following discussion, so we neglect it. The structure function  $F_2^\pi(x_\pi, Q^2)$  can be determined through a fit to experimental

data as[11][12]:

$$F_2^\pi(x, Q^2) = \frac{2}{3} f(Q^2) [a \exp(2\sqrt{L})/L + b\sqrt{x}]. \quad (16)$$

Where  $L = (4\pi/\beta_0) \ln(c/\alpha_s) \ln(d/x)$ ,  $f(Q^2) = Q^2/(e+Q^2)$ ,  $\alpha_s = 4\pi/(\beta_0 \ln(Q^2/\Lambda_{QCD}^2))$ . The resulting parameters are:  $\Lambda_{QCD} = 0.2$  GeV,  $\beta_0 = 9$ ,  $a = 0.036$ ,  $b = 0.4$ ,  $c = 0.59$ ,  $d = 0.31$ ,  $e = 0.12$  GeV<sup>2</sup>.

It is not difficult to understand why the cross section of pion-exchange is much larger than that of  $\mathbb{R}_\rho$ . Firstly, the coupling constant  $g_\pi$  is much larger than  $g_\rho$ , their ratio  $g_\pi^2/g_\rho^2 = 32.3$ . Secondly, from (14) and (16) we can see that the cross section of pion-exchange increases with the increasing of *cms* energy  $s$  ( $s \approx Q^2/x$ ), because  $F_2^\pi$  increases when  $x$  becomes smaller. On the contrary, from Regge theory the cross section of  $\mathbb{R}_\rho$ -exchange decreases quickly when  $s$  is increasing, i.e.  $\sigma \sim s^{\alpha_\rho(0)-1} = s^{-0.5}$ .

For the same reason, we can also see the large difference between pion cloud model and the  $\pi$ -Reggeon exchange, since the intercept of  $\pi$ - Reggeon is less than zero ( $\alpha_\pi(0) \approx -m_\pi^2$ ), the cross section of  $\pi$ -Reggeon exchange decreases faster than that of  $\mathbb{R}_\rho$ -Reggeon exchange, so that its contribution will be very small at high energy.

## 4 Hadronization

In the above sections, we have discussed the inclusive properties of  $\mathbb{R}_\rho$ -exchange and pion-exchange. It is more attractive to ask what can be predicted from these theories on the exclusive properties of final hadrons. Since both  $\mathbb{R}_\rho$  and pion are color singlet object, one may expect the large rapidity gap will appear in  $\eta_{max}$  distribution, here  $\eta_{max}$  is the maximum pseudo-rapidity of a event. From the theoretical point of view [11], the rapidity gap between the observed neutron and the hadronic debris can be estimated as:  $\Delta\eta \sim \ln(1/(1-z))$ . Since in  $\pi$ -exchange,  $z$  has the mean value of  $z \approx 0.7 \sim 0.9$ , so  $\Delta\eta \sim 1$ . It is very small. We will discuss this problem by using Monte Carlo method. We use Lund string fragmentation model to describe the fragmentation and hadronization process, The model has been implemented into the program JETSETS7.4 and PYTHIA5.7[15]. We use these programs to simulate the process :

$$q_u + q_{\bar{d}} \rightarrow \text{hadrons}, \quad (17)$$

which is sketched in Fig.2b, and :

$$\pi^+ + e^- \rightarrow \text{hadrons} \quad (18)$$

or :

$$\pi^+ + \gamma^* \rightarrow \text{hadrons} \quad (\text{for fixed } Q^2). \quad (19)$$

It is widely used to use the on shell pions instead of virtual pions in Monte Carlo simulation.[13]

## 5 Results and discussions

The Monte Carlo simulation was made corresponding to the HERA condition, i.e.  $E_p = 820$  GeV,  $E_e = 26.7$  GeV. For the study of the behavior under different  $x$  and  $Q^2$ , the  $\gamma^*\pi$  interaction was simulated instead of  $e\pi$  interaction from (14). We can integrate the integrand over  $dt$  and  $dz$ , then the contribution of  $\pi$ -exchange to the proton structure function  $F_{2(\pi)}^p$  can be evaluated. It is very easy from (13) to get the same contribution of  $\mathbb{R}_\rho$  exchange, and their ratio  $F_{2(\rho\text{-exchange})}^p/F_{2(\pi\text{-exchange})}^p = 0.28$  when  $x = 10^{-3}, Q^2 = 10$  GeV $^2$ . When  $x$  goes smaller, this value becomes a little bit smaller too. Note that this ratio is also the ratio of the differential cross section. From (13) we get:

$$\frac{F_{2(\rho\text{-exchange})}^p}{F_{2(\pi\text{-exchange})}^p} = \frac{d\sigma_{\gamma^*\rho}/dxdQ^2}{d\sigma_{\gamma^*\pi}/dxdQ^2}. \quad (20)$$

By using Monte Carlo method, we can get many properties of these two processes. But our special interest is in the  $\eta_{max}$  distribution. By varying  $x$  and  $Q^2$ , we get different  $\eta_{max}$  distributions of  $\mathbb{R}_\rho$ -exchange. It is shown in Fig.4 that the distribution moves down to the low  $\eta_{max}$  region when the Bjorken variable  $x$  becomes small. But in the case of  $\pi$ -exchange there is very little influence (in the region of  $10^{-4} < x < 10^{-2}, 10$  GeV $^2 < Q^2 < 100$  GeV $^2$ ).

For the comparison to the experimental data measured on FNC [16], the simulation was made under the cut:  $E_n > 400$  GeV, where  $E_n$  is the energy of the outgoing neutron. In [16] the  $\eta_{max}$  distribution of the neutron tagged events with  $E_n > 400$  GeV is given. One can find that the  $\eta_{max}$  distribution is very similar to that of normal DIS added by  $\mathbb{P}$ -exchange. But as we know, in neutron tagged events the contribution of the  $\mathbb{P}$  vanishes ( $\mathbb{P}$  has the quantum number of the vacuum). In the experiment on FNC about 3% events have large rapidity gap. It seems a little smaller than that of  $\mathbb{P}$ -exchange ( $\mathbb{P}$ -exchange gives a contribution of about 5-7% to the normal DIS). But it still need a new idea to understand it. In order to understand the source of LRG in

neutron tagged events, it is very natural to suggest that  $\mathbb{R}_\rho$ -exchange plays an important role. From the above discussion, the contribution of the  $\mathbb{R}_\rho$ -exchange to the  $\pi$ -exchange process has the magnitude of about 3%. From Fig.4 it is also very clear that  $\mathbb{R}_\rho$ -exchange events have large rapidity gap. The  $\eta_{max}$  distribution of  $\mathbb{R}_\rho$ -exchange and  $\pi$ -exchange (the  $x$  and  $Q^2$  are  $x = 0.0005, Q^2 = 50 \text{ GeV}^2$ ) are superimposed in Fig.5 where the experimental data of FNC is also given. The region of  $\eta_{max}$  shown in [16] is:  $-2.5 < \eta_{max} < 7.5$ , but the region covered by the calorimeters in ZEUS and can be really measured is  $-3.8 < \eta_{max} < 4.3$ . The values of  $\eta_{max} > 4.3$  are 'artifact' of the clustering algorithm, they are strongly affected by limited acceptance towards the forward beam hole. In order to avoid the complexity of 'artifact', the region of  $\eta_{max}$  in Fig.5 is restricted as:  $-2.5 < \eta_{max} < 4.3$ . From Fig.5 we can see that the  $\pi$ -exchange alone failed to describe the data. But together with the contribution of the  $\mathbb{R}_\rho$ -exchange, the situation becomes very different. The sum of the contributions from the two processes is shown in Fig.6. It can be seen from the figure that a very good agreement between theoretical prediction and experimental data is found.

In this paper we presented the contribution of  $\mathbb{R}_\rho$ -exchange in charge exchange process. The ratio of the cross section of  $\mathbb{R}_\rho$ -exchange process to that of  $\pi$ -exchange is obtained. We got the  $\eta_{max}$  distribution of this process by Monte Carlo simulation and compared it with that of  $\pi$ -exchange from pion cloud model. We found that neither one of the two process alone can describe the experimental data from FNC, but their sum coincides with the data very well. This shows that in studying the large rapidity gap phenomena of DIS the contribution from Reggeon exchange should be considered[4]. It is especially important in charge exchange processes.

#### **Acknowledgment:**

This work is supported in part by National Nature Science Foundation of China and the Doctoral Program Foundation of Institution of Higher Education of China. One of the author (Y.F.Zhou) is grateful to Dr. Cong-Feng Qiao for his kindly help on the calculation of  $\mathbb{R}_\rho$ -exchange, and for his helpful comments.

## References

- [1] M.Derrick et al. (ZEUS Collaboration), Phys. Lett. B315(1993)481;  
T. Ahmed et al. (H1 Collaboration), Nucl. Phys. B429(1994)477.
- [2] G. Ingelman, P.E Schlein, Phys. Lett. B152(1985)256.
- [3] A. Dommachie, P.V. Landshoff Nucl. Phys. B303(1988)634.
- [4] Hong-An Peng, Shi-Hua Zhao, Cong-Feng Qiao, Commu. Theor. Phys. 28 (1997)339.
- [5] W.Rarita et al.,Phys. Rev. 165(1968) 615.
- [6] P.D.B.Collins. An Introduction to Regge Theory And High Energy Physics (Cambridge University Press,1977).
- [7] N M C Collaboration, P.Amaudruz et al., Phys. Rev. Lett. 66 (1991) 2712.
- [8] S.Kumano, Phys. Rev. D43 (1991) 59;
- [9] J.D Sullivan, Phys. Rev. D5(1972)1732.
- [10] H.Holtman et al., Phys. Lett. B338(1994)363.
- [11] B.Kopeliovich, B.Povh, I.Potashnikova, Z. Phys. C73 (1996)131.
- [12] B.Kopeliovich, B.Povh, Phys. Lett. B367(1996)329.
- [13] M.Przybycien, A.Szczurek, G.Ingelman, DESY 96-073.
- [14] J.Pumplin, Phys. Rev. D8(1973)2249.
- [15] T.Sjöstrand, Comp. Phys. Comm. 82(1994)74.
- [16] ZEUS Collaboration, DESY 96-093.

## Figure Captions

Fig.1: The scattering processes of  $\pi + N \rightarrow \pi + N$ .

Fig.2a: The Feynman diagrams for  $\mathcal{R}_\rho$ -exchange.

Fig.2b: The process of u, d quarks fragments into hadrons.

Fig.3: Direct (Fig.a) and indirect (Fig.b) forward neutron production by  $\pi$ -exchange in the pion cloud model. The dashed line parallel to the solid line at the bottom sketches the pion cloud.

Fig.4: The  $\eta_{max}$  distribution of  $\mathcal{R}_\rho$ -exchange in different  $x$  and  $Q^2$ .

Fig.5: The  $\eta_{max}$  distribution: the dots with err bars are the experimental data from FNC, the hatched area is the  $\eta_{max}$  distribution of  $\pi^+$ -exchange, normalized to the total dimension of the data with  $\eta_{max} > 1.0$ , the solid line is the  $\eta_{max}$  distribution of  $\mathcal{R}_\rho$ -exchange.

Fig.6: The  $\eta_{max}$  distribution: the dots with err bars are the data, the solid line is the sum of the contribution of  $\pi$ -exchange and  $\mathcal{R}_\rho$ -exchange to the  $\eta_{max}$  distribution.

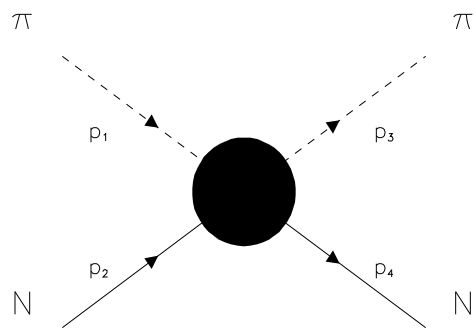


Fig.1

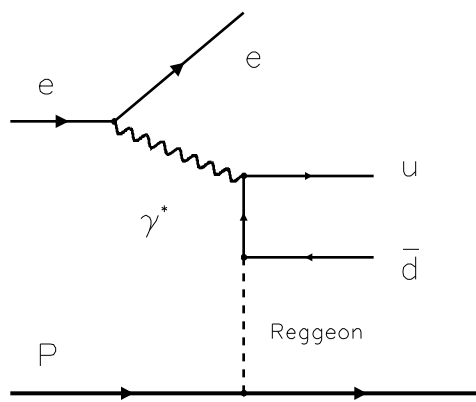


Fig.2a

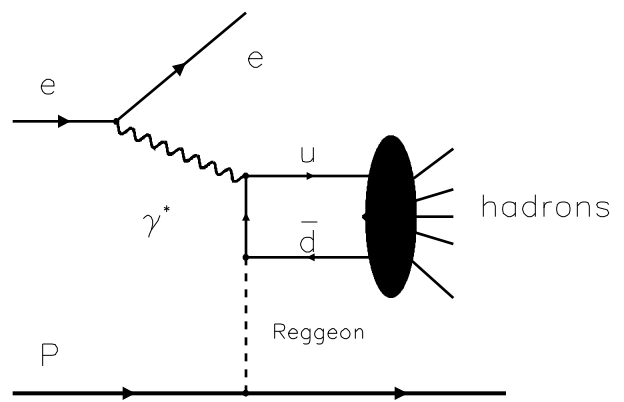


Fig.2b

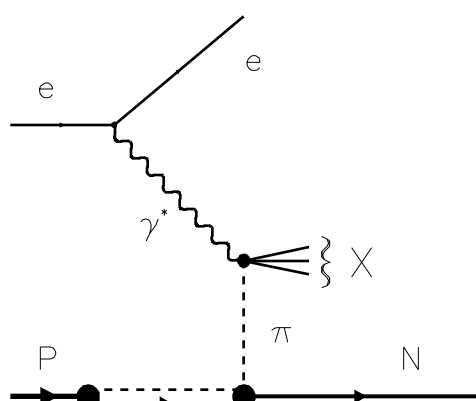


Fig.3a

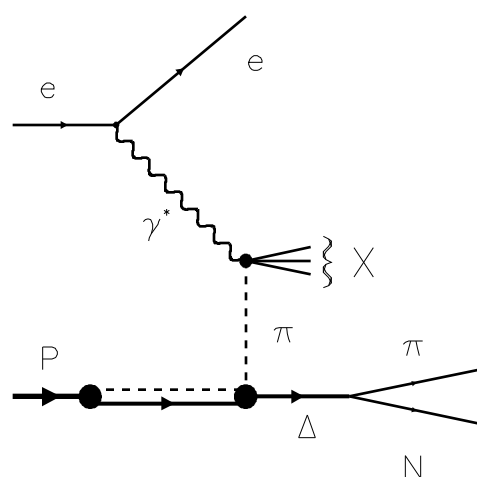


Fig.3b

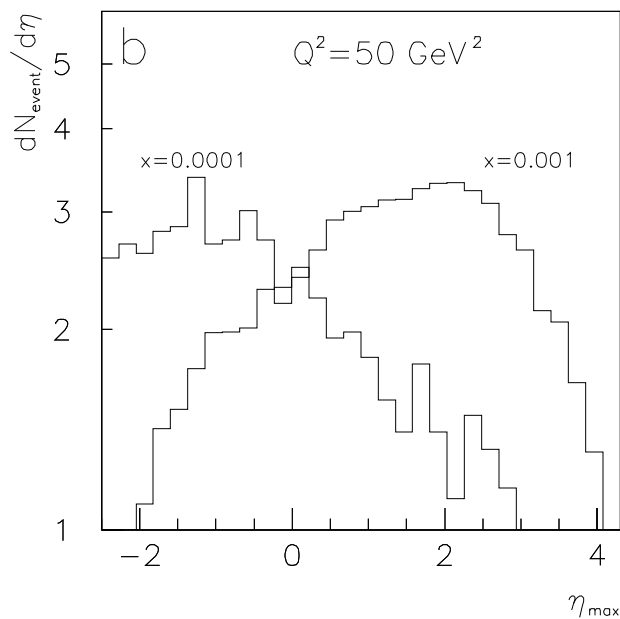
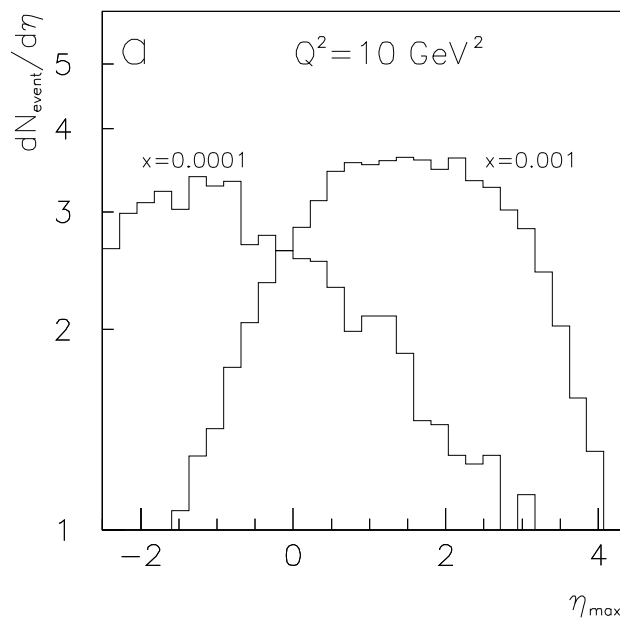


Fig. 4

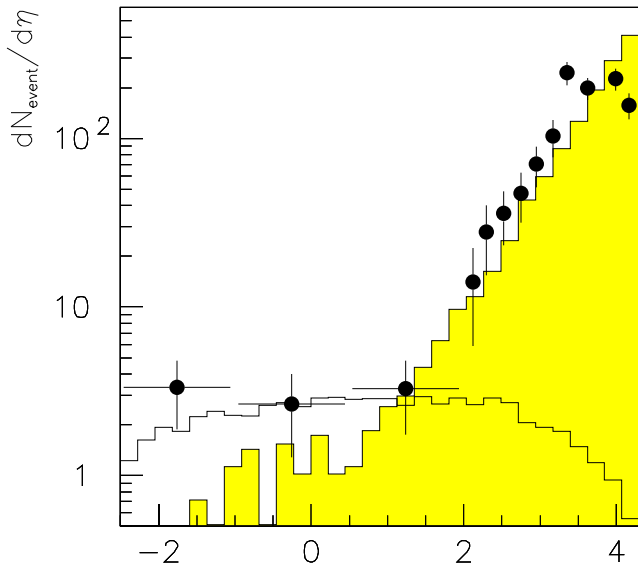


Fig. 5

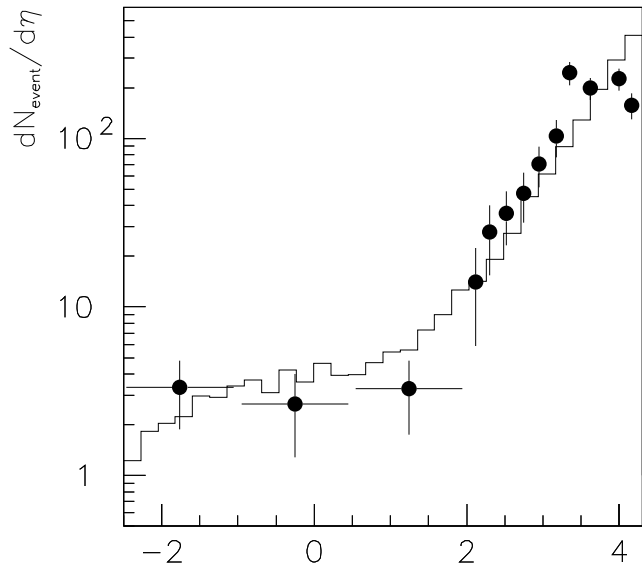


Fig. 6